Environ Geol (2007) 52:1387–1397
DOI 10.1007/s00254-006-0581-x

ORIGINAL ARTICLE

# A new approximation in determination of zonation boundaries of ignimbrite by ground penetrating radar: Kayseri, Central Anatolia, Turkey

**Tamer Koralay · Selma Kadioglu · Yusuf Kağan Kadioglu**

Received: 21 June 2006 / Accepted: 5 November 2006 / Published online: 6 December 2006


**Abstract** Ground penetrating radar (GPR) method is used as a tool to identify the zonation boundaries in ignimbrite series through their columnar section. Ignimbrites can be classified in terms of welding degree, colour, texture and mineralogical compositions. The research area comprises a part of İncesu (Kayseri) ignimbrite at Central Anatolia, Turkey. This ignimbrite is divided into three levels and each level has clear differences in terms of macroscopic and microscopic views. This paper presents the results of an application of GPR for the determination of zonation boundary within the ignimbrite flow unit in the view of their textural and petrological features. RAMAC CU II equipment was used with 250 MHz shielded antenna on parallel ten profiles to observe the physical difference among the ignimbrite levels of the study area. Two levels out of three have been defined at the İncesu ignimbrite and supported by field geology and petrographical studies. The first level, which is extremely fractured structure, is about 1.5 m thick and matches with middle level of the İncesu ignimbrite. The second level has an average 50–75 cm thickness and matches with lower level of the ignimbrite. In this manner, vertical lithological variations should be taken into consideration during petrological investigation of the ignimbrites.

**Keywords** Ignimbrite · Zonation boundary · Ground penetrating radar (GPR) · Petrography · İncesu/Kayseri

T. Koralay · Y. K. Kadioglu (✉)
Geological Engineering Department, Ankara University, Faculty of Engineering, Tandoğan 06100, Ankara, Turkey
e-mail: kadi@eng.ankara.edu.tr

T. Koralay
e-mail: koralay@eng.ankara.edu.tr

S. Kadioglu
Geophysical Engineering Department, Ankara University, Faculty of Engineering, Tandoğan 06100, Ankara, Turkey
e-mail: Kadioglu@eng.ankara.edu.tr

## Introduction

Ignimbrite is composed of the main lithology of the pyroclastic flow, which can be formed by the gravitational column collapse associated to plinian eruption from stratovolcanoes clusters and/or to the sustained fountaining of lower eruptive columns during caldera forming eruptions (Sparks and Wilson 1976; Cas and Wright 1988; Druitt 1998). This led to the classification of ignimbrites in terms of welding degree, colour, texture and mineralogical compositions. These features can be best distinguished through the columnar section than the horizontal extensions. Due to different erosion and tectonic events, some parts of the ignimbrite may be lost, which led the researcher to identify the same ignimbrite series with different definition. The study area comprises a part of the ignimbrites of Central Anatolia around İncesu Town (Kayseri, Turkey). The İncesu ignimbrite has a wide exposure with different colours and textures. Field investigations showed that they have similar colours and textures at the horizontal exposures and different colours and textures at the vertical lithology. Due to the tectonic events and erosions some parts of the ignimbrite were eroded and/or covered by young soil.

The aim of this paper is to figure out the columnar lithological changes and boundaries, of the covered and unobserved outcrops through mineralogy, petrography, and GPR method.

## Geological setting

### Regional geology

Turkey is located in the Alpine–Himalayan orogenic belt and has shown a very complex tectonic evolution during the Mesozoic and Tertiary ages. The neotectonics of Turkey is governed by three major elements. These are: the Aegean–Cyprean arc, the dextral North Anatolian Fault zone and the sinistral East Anatolian Fault Zone (Bozkurt 2001). The Central Anatolian Volcanic Province (CAVP) is located in the centre of Turkey and extends 300 km along a NE–SW direction, over a wide area (32,500 km$^2$) (Fig. 1). CAVP is composed of volcanic and volcanoclastic rocks, which are related to the collision volcanism between the Arabian and Eurasian plates, that occurred in Neogene and Quaternary (Pasquare et al. 1988).

Various researchers have investigated the Central Anatolian volcanism and its products. Pasquare (1968), Notsu et al. (1995), Aydar and Gourgaud (1998), Kürkcüoglu et al. (1998), Koralay and Kadioglu (2003) and Sen et al. (2003) dealt with the geology, petrography and geochemistry of the region. The nature and tectonic evolution of the CAVP is studied by Pasquare et al. (1988) and Toprak (1998).

The Geochronological studies reveal that the Central Anatolian volcanism started in Middle-Late Miocene and continued during late Pliocene, to the present (Innocenti et al. 1975; Schumacher et al. 1990, 2004; Le Pennec et al. 1994, 2005; Temel et al. 1998). Volcanic products of the Central Anatolia are mainly the composition of andesite and basalt.

### Geology of the study area

The study area is located35 km west of Kayseri (Turkey) and comprises the centre of the İncesu town and the vicinity (Fig. 2a). İncesu ignimbrite was first defined by Pasquare (1968) as ''İncesu member'' in Ürgüp formation. Type section of İncesu ignimbrite, which is one of the most well welded ignimbrites of the CAVP, is shown in the İncesu town. The İncesu ignimbrite is overlaid by Neogene Lake sediments with tuff intercalated and are covered by basaltic andesitic lavas (Fig. 2b). Field investigations reveal that the İncesu ignimbrite can be divided into three levels based on colour, textures, amounts of fiamme and lithic components. The typical average thickness of the İncesu ignimbrite is between 12 and 15 m (Fig. 3).

The upper level shows semi welding and has dark grey to pinkish grey colour (Fig. 4a). Thickness of upper level is approximately 2 m. The main characteristic features of the upper level are: semi welding degree, high porosity ratio, high amount of lithic fragments, and low flattening ratio of fiamme structure, which is 0.250 and in highly decomposed form. It has gradational contact with middle level. The middle level is characterized by its pinkish colour and well welding degree (Fig. 4b). It has abundant fiamme structures and angular shaped lithic fragments. The thickness of the middle level is about 7–10 m. Flattening ratio of the fiamme structures is 0.165. The middle level is differentiated from the lower level by a sharp contact

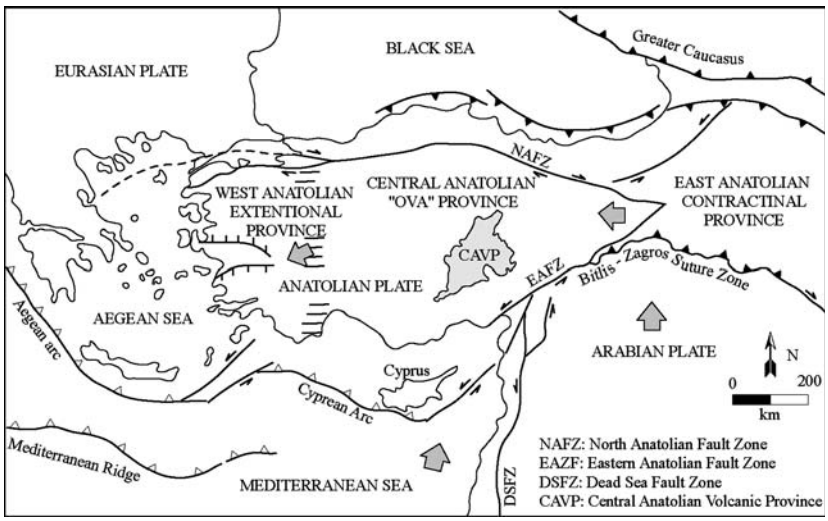


**Fig. 1** Simplified tectonic map of Turkey showing major neotectonic structures and provinces (modified from Bozkurt 2001)

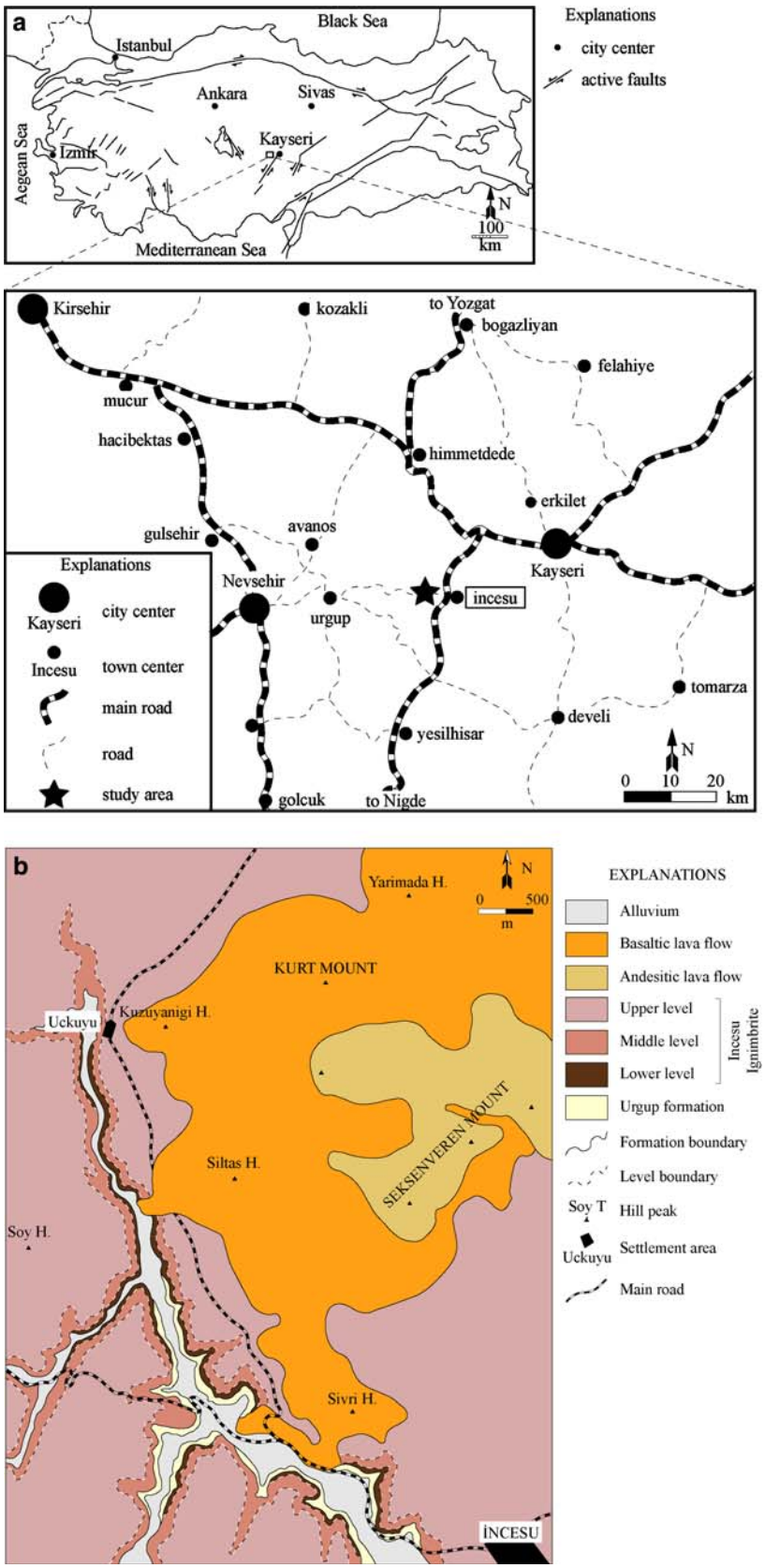


**Fig. 2** **a** Location map of the study area. **b** Geology map of the study area

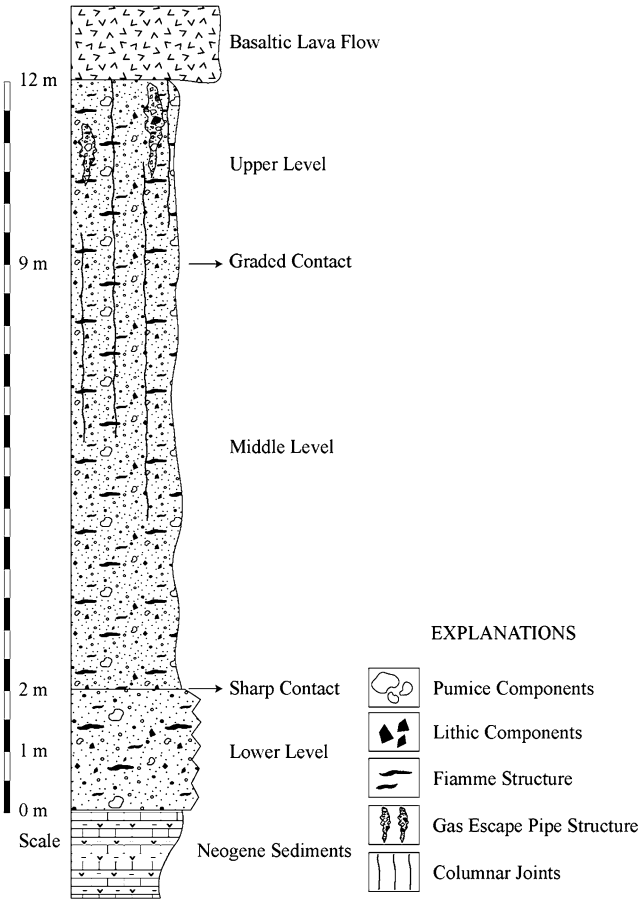


**Fig. 3** Generalized stratigraphical columnar section of İncesu ignimbrite

(Fig. 4c). The lower level isdark-brown or black coloured and has more vitreous structure than the other levels (Fig. 4d). The lower level has 2 m thickness and very dense welding degree. Flattening ratio of the fiamme structures is about 0.064.

## Petrography

The İncesu ignimbrite is composed of phenocrysts and crystal fragments, pumice and pumice fragments, shards and lithic fragments. In terms of rock forming components, the İncesu ignimbrite has vitric tuff characteristic. The amount of crystal components decreases while shard components increase from the upper to the lower level. Each level contains such phenocrysts as plagioclase, pyroxene, opaque minerals, and low amount of amphibole, biotite and quartz. In general, plagioclase and pyroxene are the most abundant phenocryst in the ignimbrite. The İncesu ignimbrite shows eutaxitic texture formed by flattened pumice fragments (fiammes) and shards. The eutaxitic texture is better developed in the lower and middle levels than in the upper level (Fig. 4e–h).

Plagioclase is one of the most frequent minerals in the ignimbrite. They are euhedral and subhedral. The size of crystals is usually 3–10 mm. The plagioclases in the upper level are more euhedral crystals and bigger in size than those in the middle and lower levels (Fig. 4e). Pyroxenes are usually thin and small subhedral crystals. They seem colourless to pale green with a very weak pleochroism (Fig. 4e).

Lithic fragments (xenoliths) are spherical, ellipsoidal and angular in shape. They have mostly andesitic and basaltic composition. There is a sharp border between lithic fragments and matrix of the ignimbrite. The pumice fragments are dark brown in colour and mostly altered to clay mineralization (Fig. 4f).

Shards are the most abundant component within the İncesu ignimbrite. They are generally small (<0.5–1 mm) particles and platy in shape. These shapes significantly change if the shards remain hot and plastic after deposition. Crystal and lithic components of the ignimbrite samples, especially those, taken from the middle or lower levels are surrounded by platy shards (Fig. 4f–h). The amounts of the shards increase from the upper level to the lower level (Fig. 4e–h).

## Ground penetrating radar

Ground penetrating radar (GPR) method, which uses electromagnetic (EM) waves, works in dielectric medium with high frequency generally between 25 and 1,600 MHz to image the subsurface. GPR is relatively new EM geophysical exploration technique that is gaining widespread use for mapping shallow subsurface geological structures and locating underground objects. GPR uses the principle of scattering of electromagnetic waves (Davis and Annan 1989). The high frequency electromagnetic wave is radiated from a transmitting antenna, travels through the material at a velocity until it hits an object or a discontinuity that has different electrical properties from surrounding medium, is scattered back to the surface and is detected by a receiving antenna. The resulting record, similar to one of the time–amplitude plots, is called as a trace. A scan is a trace, where colour scale has been applied to the amplitude values (Daniels 1989). The basic unit of the electromagnetic travel time is nanosecond (ns). GPR measurements are made by pulling the shielded antenna continuously or step by step with a constant space between transmitter and receiver unshielded antennas over the ground on a profile, or at discreet points along the surface. Traces that are displayed side

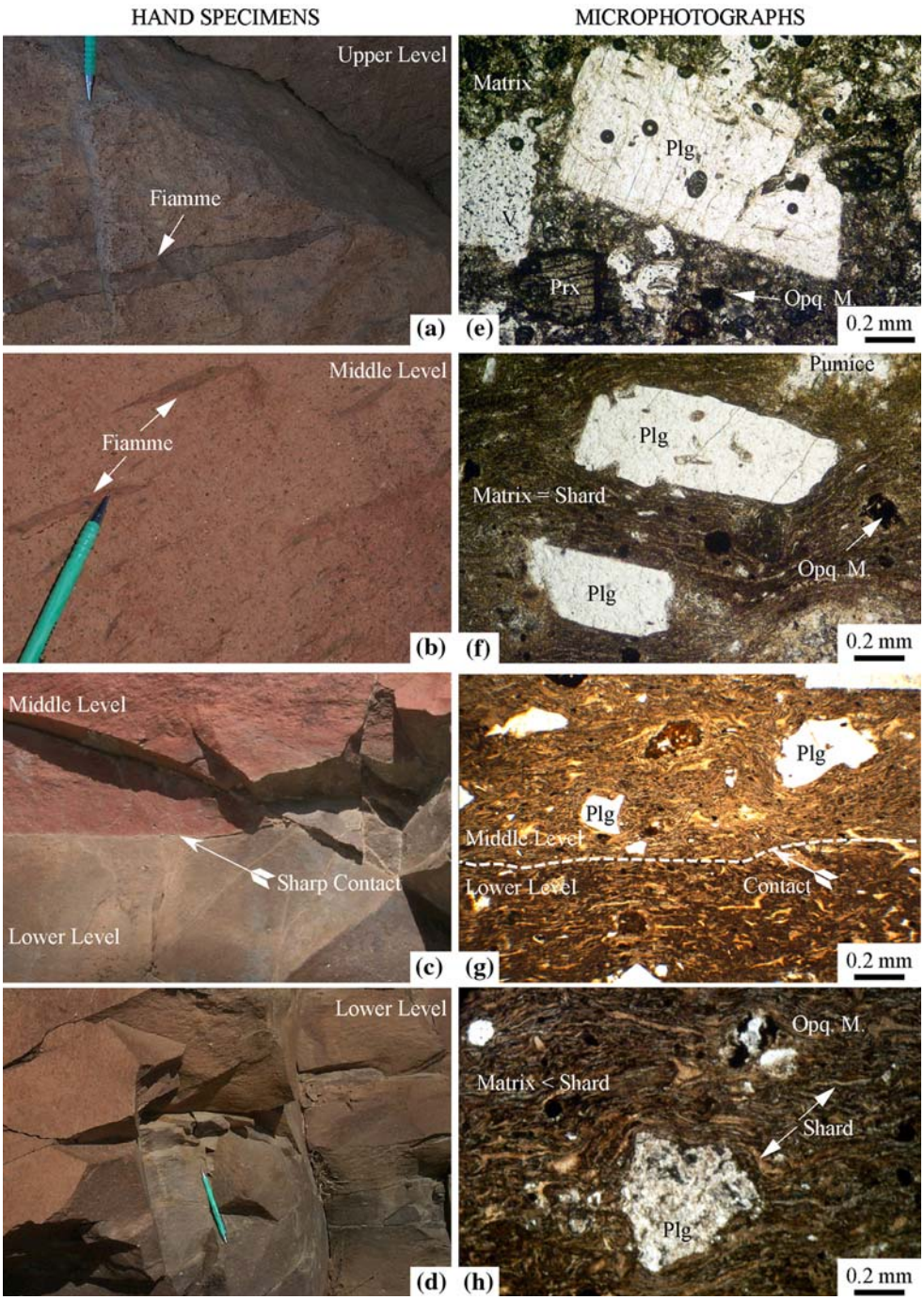


**Fig. 4** Hand specimen and microphotograph of upper, middle and lower levels of the İncesu ignimbrite (*Plg* plagioclase; *Prx* pyroxene; *Opq. M.* opaque mineral; *V* vesicule; all microphotographs are taken in plane polarized light)

by side form a GPR time-distance record, called radagram, which shows how the reflections vary in the subsurface. Therefore, its data section is very similar to a seismic reflection section. GPR time–distance record can be viewed as a 2D pseudo-image of the Earth after some processing steps, with the horizontal axis, the distance along the surface, and the vertical axis being the two-way travel time of the radar wave. The two-way travel time can be converted to depth if velocity of the medium is known. 3D visualization can be constructed from several parallel profiles by using parallel 2D profiles (Kadioglu and Daniels 2002, 2004). The 3D data volume interpretation is easier than that of 2D profiles. Because of the enhanced line to line, trace to trace, time to time correlations of reflections, it is more confident. Moreover, 3D data contain much more

information. In our approximation, a hybrid 2D/3D data collection, processing and interpretation have been done.

GPR method has been widely applied for mapping shallow stratigraphy and fractures (Benson 1995; Rust and Russell 2000; Green et al. 2003; Aldas et al. 2006), for aiding in the characterization of contaminated sites by locating buried features of interest (Kadioglu and Daniels 2002, 2004), for searching carstic cavities (Kadioglu and Ulugergerli 2004), for identifying contaminated areas where a light non-aqueous phase liquid (LNAPL) hydrocarbon has been redistributed by a rising water table in a previously hydrocarbon residual free vadose zone using GPR (Kim et al. 2000) and for identifying buried archaeological artifacts (Sambuelli et al. 1999; Cezar et al. 2001). GPR method is used for figuring out covered outcrops and characterizing the volcanic and their deposits (Russell and Stasiuk 1997; Rust and Russell 2000; Cagnoli and Ulrych 2001; Miyamoto et al. 2003; Gomez-Ortiz et al. 2006).

## Data acquisition and processing

RAMAC CU II system with 250 MHz shielded antenna, whose depth resolution is about 0.1–0.15 m and antenna separation is 0.36 m, has been used for data gathering. The study area was a horizontal platform with a size of 27 × 50 m, and ten 2D profiles, which were spaced 3 m apart, were established as parallel. Length of the profiles was 50 m. Trace spacing was 0.05 m and total time window was 193 ns with 0.377 ns time sampling interval per trace on each profile. GPR data processing was performed with Reflex-Win V3.5.

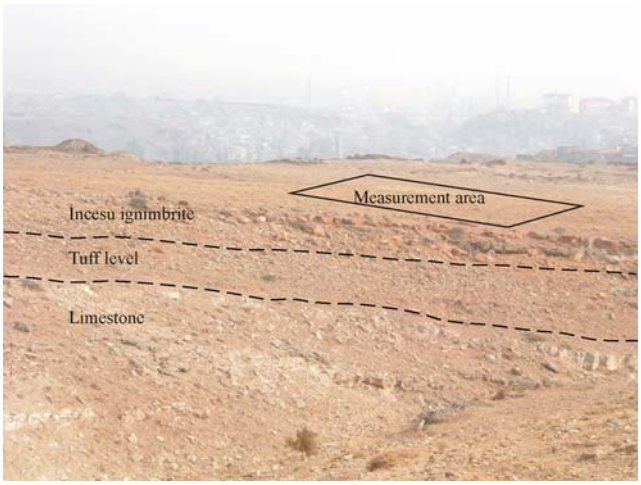


**Fig. 5** Field view of the study area showing GPR profile measurements

Figure 5 shows cross and plan view of the GPR profile measurements within the İncesu ignimbrite.

The following processing routine was applied to the collected data: zero time moving, dewow, band pass frequency filter, gain, velocity analysis, cross correlation, and diffraction stack. Topography effects were neglected because of the horizontal platform of the study area. The Reflex-Win program allows constructing a synthetic hyperbole for any given special velocity value using time–distance equation formula of EM waves to be matched with diffraction patterns throughout the profiles. The matching leads a velocity analysis. When true velocity value is found, the selected diffraction hyperbole on the profile matches with synthetic hyperbole (Gomez-Ortiz et al. 2006; Leucci and Negri 2006). The velocity analyses are realized by different diffraction hyperboles on the profiles, and then, the mean velocity is determined to transform the time scale to the depth scale. Therefore, the velocity is accepted as constant according to the depth to transform the time scale to the depth scale or to apply migration process (Rust and Russel 2000). However, this acceptance does not mean the EM wave velocity is constant vertically and laterally. The EM wave velocity ($V$) is inversely related to the dielectric constant ($K$) (Davis and Annan 1989). $K$ is related to water content and porosity of the levels. GPR reflections are caused primarily by vertical differences in the dielectric properties of levels of the medium and are given by the reflection coefficient $\mathrm{RC} = \left(\sqrt{K_1} - \sqrt{K_2}\right)/\left(\sqrt{K_1} + \sqrt{K_2}\right)$, where $K_1$ and $K_2$ are the dielectric constants of the upper layer and the lower layer of the medium, respectively (Lunt et al. 2005). If the velocity were constant, any GPR reflections would not happen on the 2D profile sections (radagrams).

In the data several hyperbolic diffractions, which allow an accurate velocity analyses, are present. Figure 6 shows a representative example of velocity analyses using the ReflexW 3.5 software. The mean velocity was determined as 0.14 m/ns for the ignimbrite (Fig. 6). This velocity was used to convert time to depth. About 73 ns (5.11 m) was used to present the 2D profile sections because the wave amplitudes attenuated in the tuff layer and terminated in the limestone.

## Results and discussion

The modal mineralogical compositions, density, porosity and humidity determinations on samples of each ignimbrite level reveal clear differences between

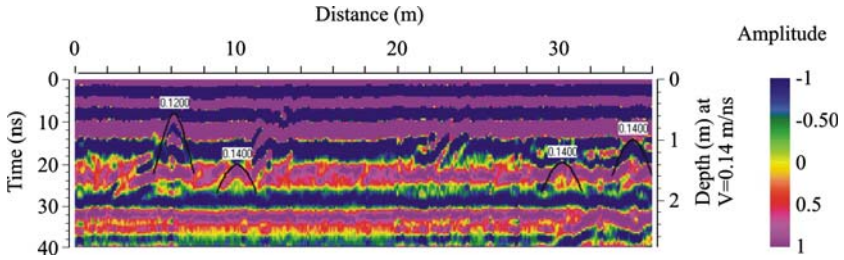


**Fig. 6** The velocity analysis on Reflex-Win V.3.5. The hyperbola matching leads a velocity analysis

**Table 1** Physical properties and modal mineralogical compositions of İncesu ignimbrite levels

| Physical properties and modal mineralogical compositions | Ignimbrite levels | | |
|---|---|---|---|
| | Upper level | Middle level | Lower level |
| Bulk density (g/cm$^3$) | 1.72 | 2.23 | 2.37 |
| Porosity (%) | 6.97 | 1.69 | 0.45 |
| Humidity (%) | 0.18–0.35 | 0.19 | 0.13 |
| Shards (%) | 5–7 | 11 | 20 |
| Xenoliths (%) | 2–5 | 4 | 6 |
| Plagioclase (%) | 2–12 | 10 | 15 |
| Mafic and opaque min (%) | 1–6 | 5 | 8 |

the levels (Table 1). The high alteration and disintegration of the upper level may cause to gain high porosity and low density with variable modal mineralogical compositions (Table 1). The results of the middle and lower levels indicated that the phenocrysts (plagioclase, mafic, and opaque minerals), xenoliths (pumice, basaltic and rhyolitic fragments) and shards increased the bulk density from the upper level toward the lower level. On the other hand, the compactions and welding of these products with volcanic ashes increased from upper level toward the lower level, leading to a decrease in the porosity with humidity ratios (Table 1).

One of the objectives of this research was to map the depth of each ignimbrite levels from the interpretation of GPR profiles. In order to monitor of these features the processed 2D profiles with their interpretation are shown in Fig. 7. Here 1.lb represents the first level boundary, which indicates the middle level of ignimbrite. 2.lb indicates the lower level of the ignimbrite and bb represents the basement boundary of the whole ignimbrite levels. The depth range of each middle and lower levels is changing from 1.2 to 1.5 m and 0.5 to 1 m, respectively. There are also some clear inclined cracks within the ignimbrite levels (profiles 1, 2 and 9 in Fig. 7).

During GPR data processing the mean velocity was determined as 0.14 m/ns for the ignimbrite (Fig. 6), while Rust and Russel (2000) used 0.09 m/ns to apply migration process and Gomez-Ortiz et al. (2006) have found that the mean velocity range of the EM waves was between 0.07 and 0.12 m/ns. The reason for the high mean velocity of the EM waves can be explained with the abundance of the shard components in the İncesu ignimbrite. Depth of the ignimbrite is about 2 m and the depth ranges of the middle level vary from 1.2 to 1.5 m. There are also some clear inclined fractures within the ignimbrite levels (profiles 1, 2 and 9 in Fig. 7) as seen in examples on hand specimens in Fig. 4a and c. The reflections of the EM waves are usually generated by any type of discontinuities, which represent differentiations of properties of the medium such as changes in the electrical properties of rocks, variations of the water content, changes in bulk density, and changes in the EM velocity or dielectric constant. The success of a GPR survey depends on a sufficient dielectric contrast to produce measurable reflection events (Gomez-Ortiz et al. 2006). Therefore, the discontinuities as faults, fractures and cracks can also be detected by GPR method (Seol et al. 2001; Orlando 2002; Porsani et al. 2006; Grasmueck et al. 2005).

Three-dimensional visualization was constructed by a series of parallel 2D profiles, starting from different profiles and depth levels, to correlate layer signatures from each profile according to depth (Figs. 8, 9). There areclear continuation boundaries between the middle (1.lb) and the lower level (2.lb). All these levels have a clear boundary between the ignimbrite and their basement (Fig. 8). Figure 9 is prepared in order to view the 3D visualizations of subsurface of the 2D profiles. Here, all boundaries are almost horizontal between the ignimbrite levels and their basement surfaces.

According to the 2D radagrams and their 3D visualizations (Figs. 7, 8, 9), three level boundaries have been observed. The first two levels belong to the middle and lower levels of the ignimbrite and the third level belongs to the tuff level of Neogene lake sediments. On above these levels, a soil unit with a thickness of 10–20 cm was interpreted as the disintegrated and decomposed products of the upper level of the İncesu ignimbrite. This level does not include in the

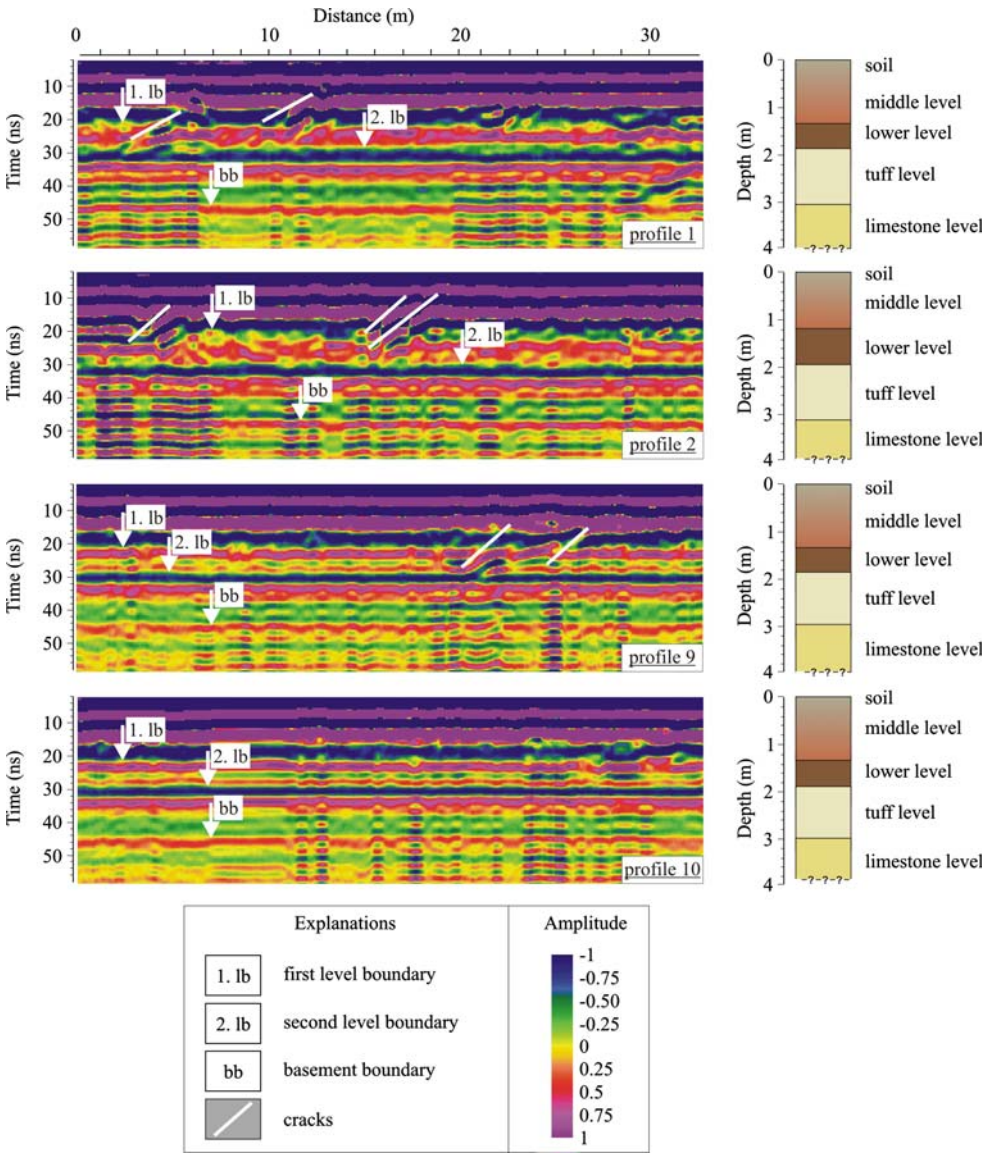


**Fig. 7** Interpreted of selected processed profiles of the measurements

GPR data processing because of their variable petrographical features and negligible thickness.

The depth of the boundary between the middle level and the lower level is 1.5 m and this boundary is seen as transitive at very small dimensions exterior one or two fractures (Figs. 7, 8, 9). When these levels are combined respectively with geology, the middle level matches with a reddish pink ignimbrite and the lower level with a blackish brown ignimbrite. The lower level is less fractured and its boundary with the tuff level is almost flat and in 2 m depths. The lower level is very thin and whose thickness is 0.5 m. The tuff level is also thin which is about 1 m and represents Neogene lake sediments, when combined with geology. Finally, all these levels are based on the limestone of the research area.

The first boundary of the İncesu ignimbrite has positive reflection (see amplitude–colour scale on Fig. 7), which means that EM wave velocity of the lower level is bigger than that of the middle level, or the dielectric constant value of the lower level is smaller than that of the middle level, according to the reflection coefficient relation with the dielectric constant ($K$) and velocity ($V$) between two levels. Moreover, the second boundary between the lower level of the ignimbrite and the tuff layer has negative reflections because the tuff layer dielectric constant is bigger than that of the lower level of the İncesu ignimbrite (Figs. 7, 8, 9).

Dielectric constant value ($K$) depends on mineral types, welding degree, flattening ratio and quantity of fiamme structure, size and amount of lithic fragment (xenoliths), porosity ratio, and humidity of a layer with

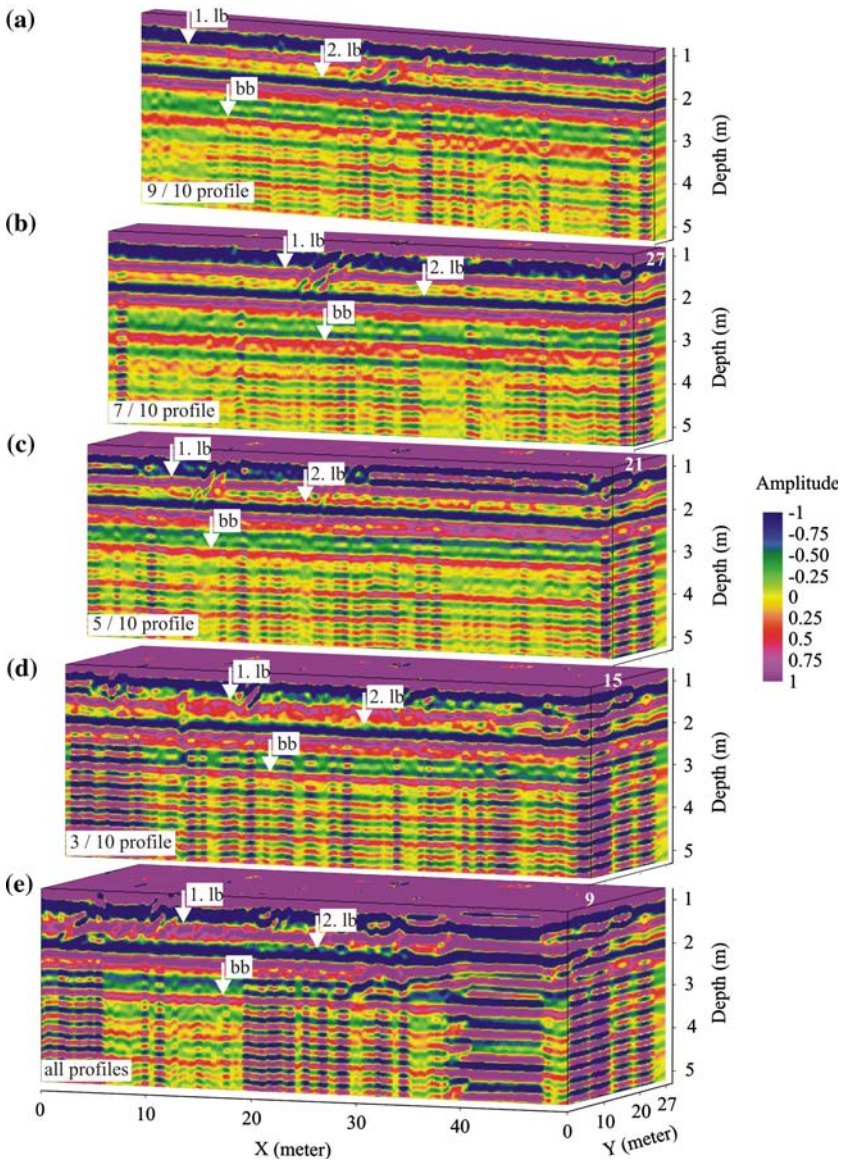


**Fig. 8** 3D visualizations of the 2D profiles including; **a** 9–10 profiles, **b** 7–10 profiles; **c** 5–10 profiles; **d** 3–10 profiles and **e** all profiles of the measurement area (*Symbols* are similar to Fig. 7)

$K_{air} = 1$ and $K_{water} = 81$. Therefore, increasing the humidity ratio causesincrease in the $K$ value anddecrease in the velocity of the layers. $K$ is inversely related to the porosity of the dry volcanic materials (Rust and Russel 2000). However, for mixing model changes in volume percentage of water will dominate changes in $K$ (Lunt et al. 2005). In addition, porosity is inversely related to the density. These relations indicate that $K$ value decreases from the middle to the lower level. The results give a positive reflection coefficient for the interface between two levels. Furthermore, the abundance of shard components in the İncesu ignimbrite decreases $K$ values of the two levels.

The variations of the petrographical features and physical properties of the ignimbrite levels causedifferent reflection signals in the radagram of the GPR profiles. As a result, GPR data can be used to determine the zonation boundaries within the ignimbrite flow unit in view of their textural and petrological features.

## Conclusions

The ignimbrite is represented by the main lithology of a pyroclastic suite and their mineral compositions and textural feature changes through the columnar sections. The welding degree, colour, texture and mineralogical compositions reveal that the İncesu ignimbrite is divided into three levels as upper, middle and lower.

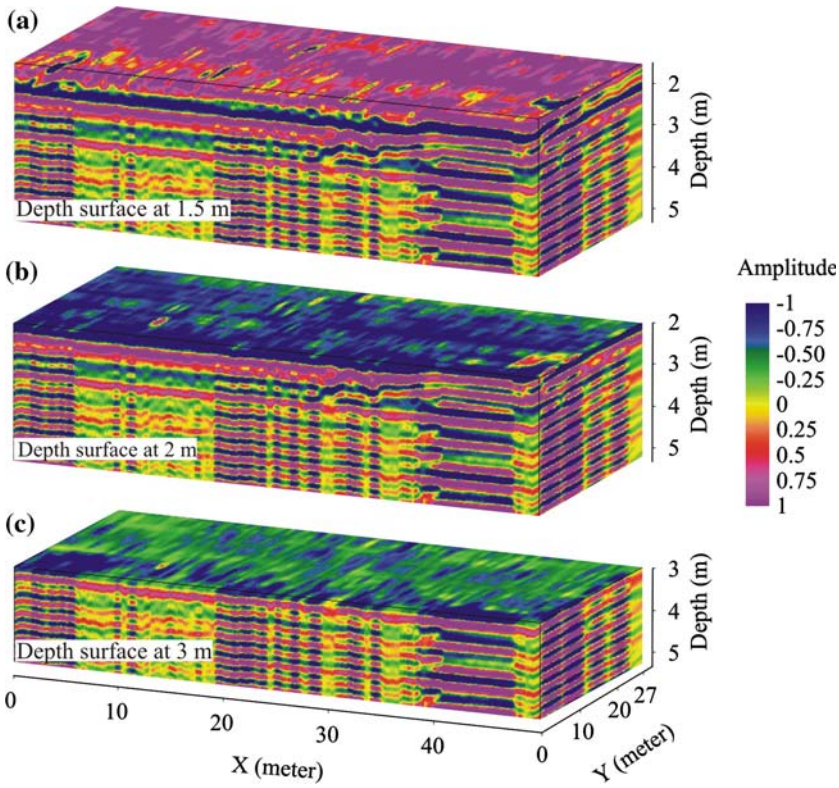


**Fig. 9** 3D visualizations of the subsurface view of the 2D profiles starting with; **a** the boundary plane of middle ignimbrite level; **b** the boundary plane of tuff level; **c** the boundary plane of limestone

Eutaxitic texture is dominant in the middle and lower level samples and these levels have more compact structure than the upper level.

Relative dielectric permittivity is active parameter in the GPR method. This parameter led to definition of the lithological unit and cracks of each unit. If there is dielectric permittivity difference between host medium and any object, or between two layers underground, then the high frequency electromagnetic wave will reflect up and reach to receiver. Therefore, this boundary can be observed on the GPR profile data. Here, if there are permittivity differences in the ignimbrite levels, GPR method can identify these levels physically.

The 2D data collection and processing were proceeded initially along a processing sequence, then a block of data was formed by combining the profile lines through the 3D view that is closely approximates an image of the subsurface, with the anomalies that are associated with the object of interest located in their special positions. The results of the GPR method supply the geological discovery according to differentiates of the dielectric permittivity parameter value, which represents a physical underground parameter in the layers. In addition, GPR method could distinguish three thin layers successfully at the study area as can be examined through the geological investigation of the zonation of the ignimbrite. The processing results of the radagrams showed that the GPR could distinguish the thin ignimbrite levels with reflected EM waves from the boundaries of different units.

**Acknowledgments** This study was financially supported by DPT 2003-K-120-190-4-1 and Scientific Research Projects Unit of the Ankara University under grant nos. 2003-07-45-015 and 2005-07-45-027. The authors would also like to extend their thanks to unknown reviewers of the manuscript for their valuable contributions.

## References

Aldas GU, Kadıoglu S, Ulugergerli E (2006) The usage of ground penetrating radar (gpr) in designing blast pattern. Rock Mech Rock Eng 39:281–290

Aydar E, Gourgaud A (1998) The geology of Mount Hasan stratovolcano, Central Anatolia, Turkey. J Volcanol Geotherm Res 85:129–152

Benson AK (1995) Applications of ground penetrating radar in assessing some geological hazards: examples of groundwater contaminants, faults, cavities. J Appl Geophys 33:177–193

Bozkurt E (2001) Neotectonics of Turkey—a synthesis. Geodinamica Acta 14:3–30

Cagnoli B, Ulrych TJ (2001) Ground penetrating radar images of unexposed climbing dune-forms in the Ubehebe hydrovolcanic field (Death Valley, California). J Volcanol Geotherm Res 109:279–298

Cas RAF, Wright JV (1988) Volcanic succession modern and ancient. Unwin Hyman, London pp 528

Cezar GS, Rocha PLF, Buarque A, Costa A (2001) Two Brezilian archeological sites investigated by GPR: Serrano and Morro Grande. J Appl Geophys 47:227–240

Daniels JJ (1989) Fundamentals of ground penetrating radar. Proceedings of SAGEEP. Golden Colorado

Davis JL, Annan AP (1989) Ground-penetrating radar for high-resolution mapping of soil and rock stratigraphy. Geophys Prospect 37:531–551

Druitt TH (1998) Pyroclastic density currents. In: JS Guilbert, RSJ Sparks (eds) The physics of explosive volcanic eruptions. J Geol Soc Lond 145:145–182

Gómez-Ortiz D, Martín-Velázquez S, Martín-Crespo T, Márquez A, Lillo J, López I, Carreño F (2006) Characterization of volcanic materials using ground penetrating radar: a case study at Teide volcano (Canary Islands, Spain). J Appl Geophys 59:63–78

Grasmueck M, Weger R, Horstmeyer H (2005) Full-resolution 3D GPR imaging. Geophysics 70:12–19

Green A, Gross R, Holliger K, Horstmeyer H, Baldwin J (2003) Results of 3-D georadar surveying and trenching the San Andreas fault near its northern landward limit. Tectonophysics 368:7–23

Innocenti F, Mazzuoli R, Pasquare G, Redicati de BF, Villari L (1975) The Neogene calc-alkaline volcanism of Central Anatolia: geochronological data of Kayseri–Nigde area. Geol Mag 112:349–360

Kadioglu S, Daniels JJ (2002) A hybrid 2d/3d ground penetrating radar (gpr) survey of brownfield site along Lake Street in Chicago, Illinois (USA). In: International conference on Earth sciences and electronics 2002 (ICESE-2002), vol 2, pp 255–261

Kadioglu S, Daniels JJ (2004) Integrated 3D visualization of GPR data and EM-61 data. Geochim Cosmochim Acta 68(11):A468

Kadıoğlu S, Ulugergerli EU (2004) Determination of cavities using ground penetrating radar in Dalaman-Akköprü dam construction Area. The sixteenth international geophysics congress and exhibition of Turkey, Abstract book 372–375

Kim C, Daniels JJ, Guy E, Radzevicius SJ, Holt J (2000) Residual hydrocarbons in a water-saturated medium: a detection strategy using ground penetrating radar. Environ Geosci 7(4):169–176

Koralay T, Kadioglu YK (2003) Petrographic determination of top and botoom levels of ignimbrites: İncesu (Kayseri) ignimbrite. J Fac Eng Arch Selcuk Univ 18:43–54

Kürkcüoglu B, Sen E, Aydar E, Gourgaud A, Gündoğdu N (1998) Geochemical approach to magmatic evolution of Mt. Erciyes stratovolcano Central Anatolia, Turkey. J Volcanol Geotherm Res 85:473–494

Le Pennec JL, Bourdier JL, Froger JL, Temel A, Camus G, Gourgaud A (1994) Neogene ignimbrites of the Nevsehir plateau (Central Turkey): stratigraphy, distribution and source constraints. J Volcanol Geotherm Res 63:59–87

Le Pennec JL, Temel A, Froger JL, Sen S, Gourgaud A, Bourdier JL (2005) Stratigraphy and age of the Cappadocia ignimbrites, Turkey reconciling field constraints with paleontologic, radiochronologic, geochemical and paleomagnetic data. J Volcanol Geotherm Res 141:45–64

Leucci G, Negri S (2006) Use of ground penetrating radar to map subsurface archaeological features in an urban area. J Archaeol Sci 33:502–512

Lunt IA, Hubbard SS, Rubin Y (2005) Soil moisture content estimation using ground-penetrating radar reflection data. J Hydrol 307:254–269

Miyamoto H, Haruyama J, Rokugawa S, Onishi K, Toshioka T, Koshinuma J (2003) Acquisition of ground penetrating radar data to detect lava tubes: preliminary results on the Komoriana cave at Ruji volcano in Japan. Bull Eng Geol Env 62:281–288

Notsu K, Fujitani T, Ui T, Matsuda J, Ercan T (1995) Geochemical features of collision-related volcanic rocks in central and eastern Anatolia, Turkey. J Volcanol Geotherm Res 64:171–192

Orlando L (2002) Ground penetrating radar in massive rock: a case history. Eur J Environ Eng Geophys 7:265–279

Pasquare G, (1968) Geology of the Cenozoic volcanic area of Central Anatolia. Atti Accad Naz Lincei Mem 9:55–204

Pasquare G, Poli S, Vezzoli L, Zanchi A (1988) Continental arc volcanism and tectonic setting in Central Anatolia, Turkey. Tectonophysics 146:217–230

Porsani JL, Sauck WA, Junior AOS (2006) GPR for mapping fractures and as a guide for the extraction of oranamental granite from a quarry. A case study from southern Brazil. J Appl Geophys 58:177–187

Russell JK, Stasiuk MV (1997) Characterization of volcanic deposits with ground penetrating radar. Bull Volcanol 58:515–527

Rust AC, Russell JK (2000) Detection of welding in pyroclastic flows with ground penetrating radar: insights from field and forward modelling data. J Volcanol Geotherm Res 95:23–34

Sambuelli L, Socco LV, Brecciaroli L (1999) Acquisition and processing of electric, magnetic and GPR data on a Roman site (Victimulae, Salussola, Biella). J Appl Geophys 41:189–204

Schumacher R, Keller J, Bayhan H (1990) Depositional characteristics of ignimbrites in Cappadocia, Central Anatolia, Turkey. In: Savaşçın MY, Eronat AH (eds) Proceedings of the international Earth science congress on Aegean regions (IESCA 1990), vol 2, pp 435–449

Schumacher UM, Schumacher R, Götte-Viereck GL, Lepetit P (2004) Areal distribution and bulk rock density variations of the welded incesu ignimbrite, Central Anatolia, Turkey. Turk J Earth Sci 13:249–267

Sen E, Kürkcüoğlu B, Aydar E, Gourgaud A, Vincent PM (2003) Volcanological evolution of Mount Erciyes stratovolcano and origin of the Valibaba Tepe ignimbrite (Central Anatolia, Turkey). J Volcanol Geotherm Res 125:225–246

Seol SJ, Kim JH, Song Y, Chung SH (2001) Finding the strike direction of fractures using GPR. Geophys Prospect 49:300–308

Sparks RSJ, Wilson L (1976) A model for the formation of ignimbrites by gravitational column collapse. J Geol Soc Lond 132:441–451

Temel A, Gündoğdu MN, Gourgaud A, Le Pennec JL (1998) Ignimbrites of Cappadocia (Central Anatolia, Turkey): petrology and geochemistry. J Volcanol Geotherm Res 85:447–471

Toprak V (1998) Vent distribution and its relation to regional tectonics, Cappadocian Volvanics, Turkey. J Volcanol Geotherm Res 85:55–67